Pedestal particle transport during the ELM cycle at ASDEX Upgrade

E. Wolfrum[1], F.M. Laggner[2], S. Keerl[2], J. Gnilsen[2], G. Birkenmeier[1], E. Fable[1], L. Guimarais[3], F. Mink[1], the EUROfusion MST1 Team* and the ASDEX Upgrade Team

[1] Max-Planck-Institute for Plasma Physics, 85748 Garching, Germany, [2] Institute of Applied Physics, TU Wien, Fusion@ÖAW, 1040 Vienna, Austria, [3] Instituto de Plasma e Fusao Nuclear, Instituto Superior Tecnico, Unversidade de Lisboa, Portugal

Edge localized modes (ELMs) appear in plasmas with steep pressure gradients in the edge transport barrier. During an ELM crash the edge pressure relaxes, while heat and particles are transported into the scrape-off layer (SOL) and to the divertor. Subsequently, the recovery of the edge profiles of electron density (n_e), electron temperature (T_e) and ion temperature (T_i) occurs on well separated time scales which have different durations [1,2,3]. The various phases of the edge pedestal recovery are correlated with distinct signatures in the magnetic signals at the mid-plane [2,4], changes in divertor conditions [5] and changes in the SOL density at the high field side and the low field side [6].

A prominent feature of the inter-ELM pedestal development is the very fast recovery of the pedestal top n_e and T_i, which both occur before T_e recovers. This behaviour has been found to be universal at ASDEX Upgrade, i.e. at different collisionalities [2], for different isotope species [7] and also for different plasma shapes [8]. The pedestal density behaviour is a complex interplay of transport and sources. The divertor neutrals and the high field side high density (HFSHD) region [9,10] influence the separatrix density. The SOL profiles determine the transparency to neutrals and thus the ionisation source profile inside the separatrix, which influences the gradient. Last but not least instabilities in the pedestal affect particle transport.

In this work, ELM resolved data at the mid-plane and in the divertor are analysed for an exemplary ELM cycle. The measured profiles are modelled by the transport code ASTRA [11] in order to determine whether a diffusively described particle transport changes during the ELM cycle. The neutral source profile is not experimentally accessible and is therefore modelled by four different temporal evolutions during the ELM cycle, taking into account midplane or divertor SOL data. Also the energy of the neutral particles is changed so that the modelling results can provide a comprehensive picture of the uncertainties of the obtained diffusion coefficients.

Figure 1a) shows the ELM synchronised spectrogram of the ASDEX Upgrade plasma discharge #30701 (B_t = -2.5T, I_p = 1 MA, P_{tot} = 5 MW) from t = 2.975 s to t = 3.4 s, a phase with similar ELMs at a frequency of 70 Hz. The ELM cycle can be divided into distinct phases corresponding to the magnetic fluctuations. After the ELM crash, which is characterised by a broadband fluctuation from 0 - 1.5 ms, the quiet phase I occurs in which no magnetic fluctuations are observed except for the low frequency ones originating from a core mode. In phase II mid-frequency fluctuations appear with frequencies of 50 - 150 kHz which might be responsible for additional particle transport into the SOL, visible as increased D_α signal at the divertor and an increase in the target electron density [12]. The onset of high-frequency fluctuations (180 - 250 kHz) characterises phase III, when both n_e and T_e reach pre-ELM values. While the phases called ELM, I and II are very similar in duration for each ELM cycle, the temporal length of phase III can vary by a few ms and is thus responsible for the scatter in ELM frequency.

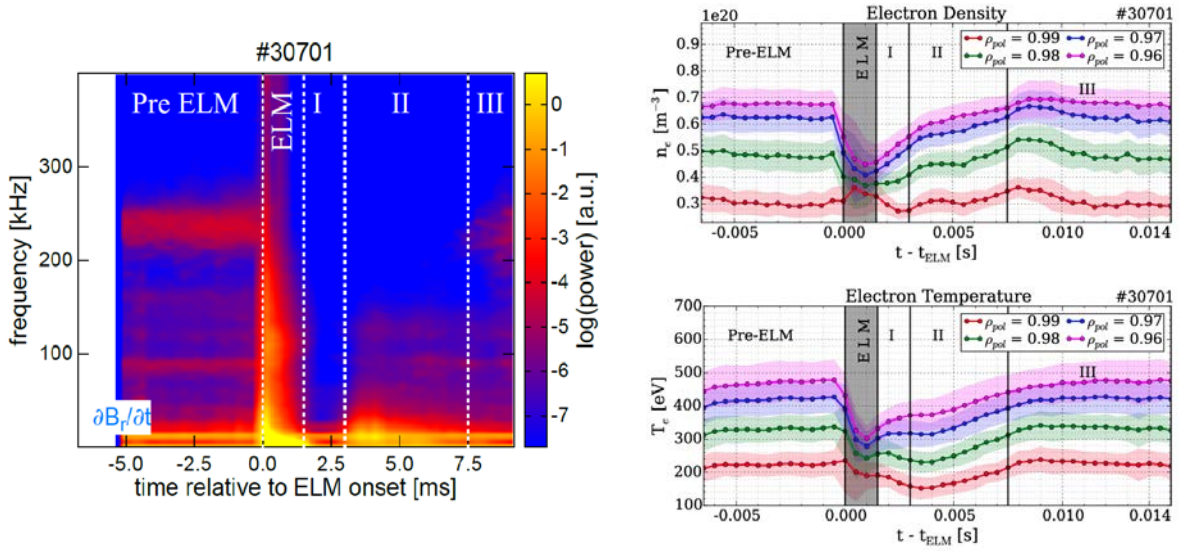

Figure 1: a) ELM synchronised magnetic histogram of 31 ELM cycles in discharge #30701, t = 2.975-3.4 s. b) Electron density and c) electron temperature evolution relative to the ELM onset for ρ_{pol}=0.97, 0.98 and 0.99.

In figures 1b) and 1c) the evolution of the edge n_e and T_e profiles are shown. After the reduction in both value and gradient during the ELM, a fast steepening of the n_e profile can be observed in phase I, in which the T_e profile only marginally changes. It is one purpose of this work to determine the origin of the fast n_e increase after the ELM crash.

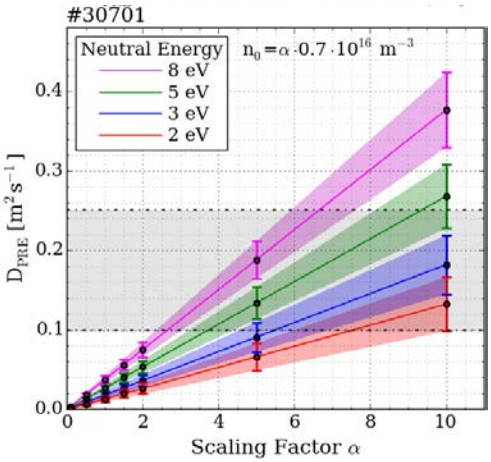

Figure 2:
Diffusion coefficient in the pre-ELM phase, D_{PRE}, calculated by ASTRA for an independent variation of the neutral density $\alpha \cdot n_0$ and the neutral energy. The grey shaded area corresponds to diffusion coefficients determined in reference [13].

The 1.5D transport code ASTRA [11] is used in an interpretive way, i.e. the measured profiles are prescribed with a temporal resolution of 0.5 ms and the temporal evolution of the purely diffusive particle transport coefficients are calculated to match the measurements. A mono-energetic neutral density at the separatrix is an input parameter to the subroutine NEUT, which provides a neutral source profile across the pedestal taking into account the measured n_e and T_e profiles. We varied the absolute magnitude of the neutral density (represented by a scaling factor α as multiplier to an arbitrary value of $n_{0,a}=0.7 \cdot 10^{16}$ m^{-3}) as well as the energy of the neutral particles between 2 and 8 eV. The calculated pedestal diffusion coefficients for the pre-ELM phase, D_{PRE}, are summarised in figure 2.
For all energies there is a linear dependency of D_{PRE} on the neutral particle density $\alpha \cdot n_{0,a}$: a higher ionisation source must be compensated by increased diffusion in order to model the same measured profiles. The same holds true for higher neutral energies, because at the same

density higher energies correspond to a larger particle flux across the separatrix. From figure 2 it becomes immediately clear, that a reliable particle diffusion coefficient can only be calculated if both, density and energy composition of neutrals at the separatrix are known, which can vary not only poloidally but also toroidally [14]. For an estimation of the temporal variation of the neutral density at the separatrix we tested four different cases: (A) constant n_0, (B) the ELM synchronised neutral particle flux at the mid-plane just behind a limiter (figure 3a), data are shifted by -1.5 ms to take into account the delay of the measurement with respect to the particles arriving at the limiter) was taken as input to KN1D [15] calculations delivering particle densities at the separatrix, (C) the temporal evolution of the ELM synchronised D_α signal in the outer divertor (figure 3b)) was used as a proxy for the neutral density at the separatrix, (D) as (C) but with reduction during the ELM phase and phase I assuming that the high density plasma in the divertor during and immediately after the ELM is not transparent to neutrals.

Figure 4 shows examples of ASTRA results for two different runs, in which $\alpha = 8$ and $E = 3$ eV was chosen. Figure 4a) shows the results for case (B). During phase I the diffusion coefficient is increased when compared to the pre-ELM phase, while in phases II and III no change in the average values (black symbols) can be observed. In figure 4b) the neutrals are modelled from the divertor D_α signal (case (D)). In phase I, D does not exhibit a significant increase in this case but also no reduction. Phase II, which is the phase with the mid-frequency fluctuations, shows an augmentation of D by roughly a factor of 3 when compared to phase III (high frequency fluctuations).

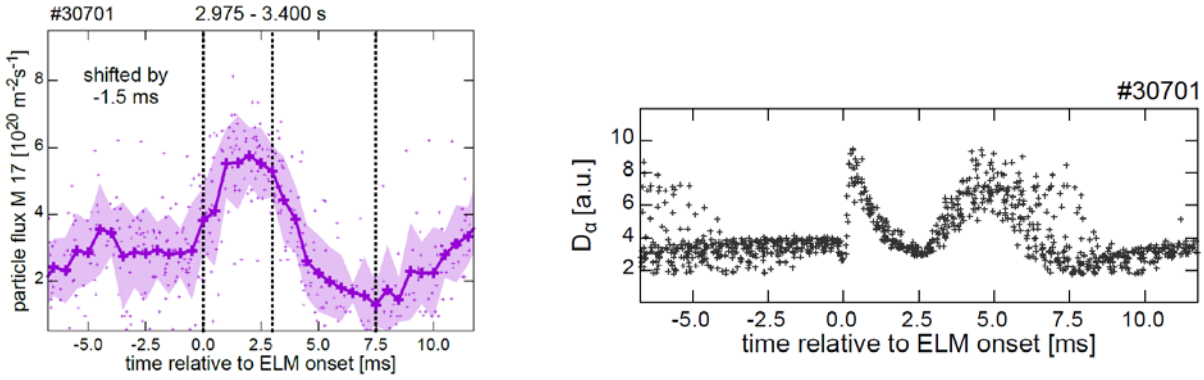

Figure 3: Temporal evolution during the ELM cycle of a) neutral particle flux at the mid-plane in the limiter shadow and b) D_α signal in the outer divertor.

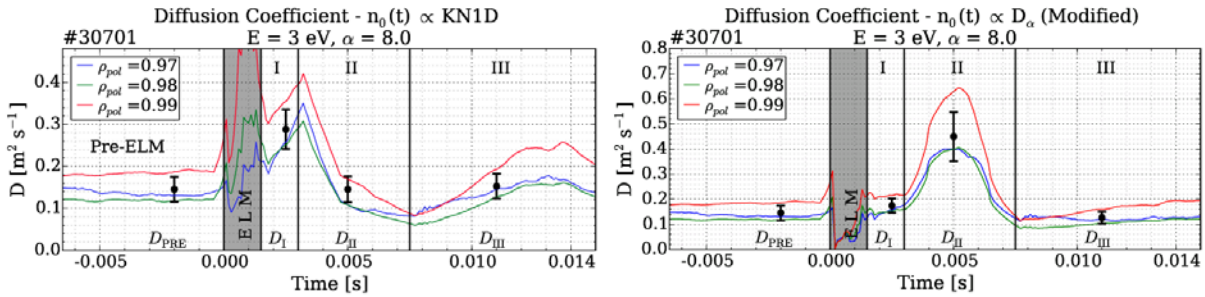

Figure 4: ASTRA output for the temporal development of the diffusion coefficient D during the ELM cycle at three radial locations in the pedestal region for neutral density estimated from a) mid-plane and b) divertor data.

A summary of these results is visualised in figure 5 for the different ELM cycle phases and for the four different temporal models for the neutral density at the separatrix.

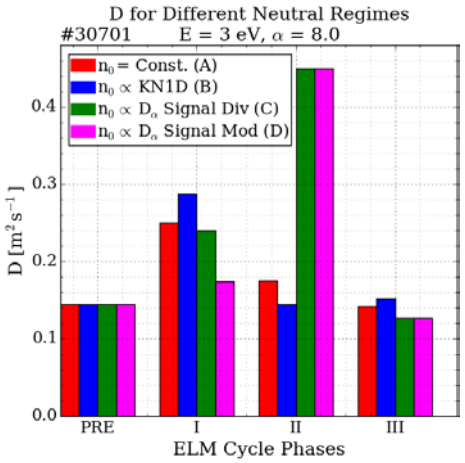

Figure 5: Average pedestal diffusion coefficient for the different phases during the ELM cycle. The bars denote the tested temporal evolutions of the neutral density at the separatrix: a constant density (A, red), calculated from mid-plane particle flux (B, blue), proportional to D_α signal in the outer divertor (C, green), same as C but with divertor assumed opaque to neutrals during the ELM phase and during phase I (D, magenta).

The results of phase I, in which the density rises quickly, suggests for all cases that in this phase the diffusion coefficient is not reduced, although there is no activity in the magnetics. It can be shown that the timescales of the changes in the inner divertor, the HFSHD region and the main chamber neutral fluxes do not fit the timescale of the n_e recovery [12]. Therefore, the fast n_e recovery can be attributed to a reduced particle flux due to the reduced gradient. The pedestal builds up because of the continuous flux from the core and a reduced flux across the separatrix. In phase II the particle flux increases again correlated with the appearance of magnetic fluctuations in the pedestal, causing the pedestal top density to saturate and giving rise to an additional particle flux to the divertor. The higher particle flux in the divertor in phase II could be due to the steep gradients only, but also because of an increased D related to the mid-frequency fluctuations. The appearance of high frequency fluctuations in phase III does not change D. Note, however, that the absolute value of the diffusion coefficient can only be determined if the poloidally averaged neutral particle flux across the separatrix is known.

Acknowledgement:
This work has been carried out within the framework of the EUROfusion Consortium and has received funding from the Euratom research and training programme 2014-2018 under grant agreement No 633053. The views and opinions expressed herein do not necessarily reflect those of the European Commission.

References:

[1] Burckhart et al, PPCF 52 (2010) 105010
[2] Laggner et al, PPCF 58 (2016) 065005
[3] Cavedon et al, to be published
[4] Mink et al, PPCF 58 (2016) 125013
[5] Wischmeier et al, JNM 363–365 (2007) 448
[6] Guimarais et al, EPS 2015
[7] Laggner et al, PoP 24 (2017) 056105
[8] Laggner et al, EPS 2015
[9] Potzel et al JNM 463 (2015) 541
[10] Reimold et al, NME 2017
[11] Pereverzev, IPP Reports 5/98, 2002
[12] Laggner et al, submitted to PPCF
[13] Chankin et al, PPCF 48 (2006) 839
[14] Lunt et al, PPCF 59 (2017) 055016
[15] LaBombard, Massachusetts Institute of Technology, Cambridge USA, 2001

*See the author list of “Overview of progress in European Medium Sized Tokamaks towards an integrated plasma-edge/wall solution” by H. Meyer et al., accepted for publication in Nuclear Fusion.